

# Biosorption and degradation of decabromodiphenyl ether by *Brevibacillus brevis* and the influence of decabromodiphenyl ether on cellular metabolic responses

Linlin Wang<sup>1</sup> · Litao Tang<sup>1</sup> · Ran Wang<sup>1</sup> · Xiaoya Wang<sup>1</sup> · Jinshao Ye<sup>1</sup> · Yan Long<sup>1</sup>

Received: 2 June 2015 / Accepted: 3 November 2015 / Published online: 10 November 2015  
© Springer-Verlag Berlin Heidelberg 2015

**Abstract** There is global concern about the effects of decabromodiphenyl ether (BDE209) on environmental and public health. The molecular properties, biosorption, degradation, accumulation, and cellular metabolic effects of BDE209 were investigated in this study to identify the mechanisms involved in the aerobic biodegradation of BDE209. BDE209 is initially absorbed by wall teichoic acid and N-acetylglucosamine side chains in peptidoglycan, and then, BDE209 is transported and debrominated through three pathways, giving tri-, hepta-, octa-, and nona-bromodiphenyl ethers. The C–C bond energies decrease as the number of bromine atoms on the diphenyl decreases. Polybrominated diphenyl ethers (PBDEs) inhibit protein expression or accelerate protein degradation and increase membrane permeability and the release of  $\text{Cl}^-$ ,  $\text{Na}^+$ ,  $\text{NH}_4^+$ , arabinose, proteins, acetic acid, and oxalic acid. However, PBDEs increase the amounts of  $\text{K}^+$ ,  $\text{Mg}^{2+}$ ,  $\text{PO}_4^{3-}$ ,  $\text{SO}_4^{2-}$ , and  $\text{NO}_3^-$  assimilated. The biosorption, degradation, accumulation, and removal efficiencies when *Brevibacillus brevis* ( $1 \text{ g L}^{-1}$ ) was exposed to

BDE209 ( $0.5 \text{ mg L}^{-1}$ ) for 7 days were 7.4, 69.5, 16.3, and 94.6 %, respectively.

**Keywords** Bioaccumulation · Biotransformation · Metabolism · Polybrominated diphenyl ether · Cell wall · ChemOffice

## Introduction

The use of certain polybrominated diphenyl ethers (PBDEs) in various industries has been prohibited because PBDEs are toxic and are ubiquitous, persistent, and accumulative in the environment (Johansson et al. 2011). More decabromodiphenyl ether (BDE209) than other PBDEs has been used, and it is the predominant PBDE congener in the environment and biota around the world (Guardia et al. 2012; Tian et al. 2012). Concern about the effects BDE209 can have on the environment and public health is growing. It is therefore important that as much BDE209 as possible is removed from water, sediment, and biota.

Various microorganisms and animals can transform PBDEs into less brominated products, and such biodegradation is an excellent way of degrading and then removing PBDEs from the environment (Lee et al. 2011). Investigations into the natural biodegradation of PBDEs have mainly been focused on identifying the pathways involved in biodebromination under anaerobic conditions (Rayne et al. 2003; Yen et al. 2009). Electron donors, such as acetate, ethanol, hydrogen, lactate, methanol, and pyruvate, and other supplements have been added to treatment systems to increase the biodegradation rate because microbial consortia and species such as *Dehalococcoides* and *Dehalobacter* that can degrade PBDEs and that thrive under anaerobic conditions are strict autotrophs (He et al. 2006; Qiu et al. 2012; Robrock et al. 2008). However, autotrophic debromination tends to take a long time to occur because

Responsible editor: Roland Kallenbom

**Electronic supplementary material** The online version of this article (doi:10.1007/s11356-015-5762-2) contains supplementary material, which is available to authorized users.

✉ Jinshao Ye  
jsye@jnu.edu.cn; folaye@126.com

✉ Yan Long  
dragonflamely@163.com

<sup>1</sup> Research Center of Environmental Pollution Control and Remediation of Guangdong Province, Key Laboratory of Environmental Exposure and Health of Guangzhou City, School of Environment, Jinan University, Guangzhou, Guangdong 510632, China

autotrophs have low growth rates. For example, less than 20 % of the PBDEs present in one study were found to have been degraded by anaerobic bacteria after 70 days (Yen et al. 2009). Furthermore, the low efficiencies at which metabolites are degraded under anaerobic conditions could mean that toxic metabolites accumulate. Highly halogenated xenobiotics were previously considered to be resistant to aerobic transformation, and BDE209 was once thought not to be bioavailable, but these assumptions were abandoned when BDE209 was found to be effectively degraded by *Pseudomonas aeruginosa* and *Phlebia lindtneri* (Shi et al. 2013; Xu and Wang 2014).

The biodegradation of BDE209 is metabolically mediated. A thorough exploration of the mechanisms involved in the biodegradation of BDE209 requires the links among cellular metabolism; the molecular properties of BDE209; and the biosorption, degradation, and transformation of BDE209 under aerobic conditions to be identified. Understanding the mechanisms involved will improve our ability to use the biodegradation of BDE209 to remediate polluted environments. Biosorption is one of the first processes that occur during the degradation process, so it may be the rate-limiting step. Biosorption is primarily dependent on the topological structures of and the physicochemical relationships between BDE209 and the cellular peptidoglycan layers. Excessive changes to the peptidoglycan structure caused by PBDEs could trigger cellular apoptosis, but a lack of affinity between the PBDEs and the cellular surface would limit the degree to which the PBDEs will be absorbed and transported. It is therefore necessary to investigate the binding of PBDEs to the cell surface to allow the degradation mechanism that occurs in the cell to be identified.

*Brevibacillus brevis* has been isolated from contaminated sediment samples from Guiyu, Guangdong Province, China (Ye et al. 2013a). These samples contained high concentrations of heavy metals, organotin compounds, polycyclic aromatic hydrocarbons, and PBDEs. It has been found that *B. brevis* can degrade BDE209, furalaxyl, metalaxyl, poly(vinyl alcohol), pyrene, and triphenyltin (Kim and Yoon 2010; Sulimma et al. 2013). The optimal conditions for the degradation of BDE209 by *B. brevis* in the presence of tea saponin have been determined (Tang et al. 2014).

The study presented here was performed to improve the understanding of BDE209 degradation by *B. brevis* through identifying the relationships among the molecular properties of PBDEs, the binding of BDE209, the transformation of BDE209, and the cellular metabolic responses to BDE209. Relationships between the transformations of different metabolites and the molecular properties of the metabolites were identified using molecular calculations. The cellular metabolic responses were characterized by monitoring the  $\text{Na}^+$ ,  $\text{NH}_4^+$ ,  $\text{K}^+$ ,  $\text{Mg}^{2+}$ ,  $\text{Cl}^-$ ,  $\text{PO}_4^{3-}$ ,  $\text{SO}_4^{2-}$ ,  $\text{NO}_3^-$ , arabinose and organic acid metabolisms, the cellular membrane permeability, nutrient use activity, and protein concentration.

## Materials and methods

### Strain and chemicals

*B. brevis* was proved to be an aerobic strain through physicochemical experiments and was preserved in the laboratory of the School of Environment at Jinan University. It was also stored at the Guangdong Microbiology Culture Centre (GDMCC) as GIMCC1.825. BDE209 was purchased from Sigma Aldrich (St. Louis, MO, USA). The concentrations of beef extract, peptone, NaCl, and  $\text{MgSO}_4 \cdot 7 \text{H}_2\text{O}$  in the culture medium were 3, 10, 5, and  $0.05 \text{ g L}^{-1}$ , respectively. The BDE209 treatment solution contained (in  $\text{mg L}^{-1}$ ) the following: 100  $\text{Na}_2\text{HPO}_4 \cdot 12 \text{H}_2\text{O}$ , 30  $\text{KH}_2\text{PO}_4$ , 50 NaCl, 20  $\text{NH}_4\text{NO}_3$ , 10  $\text{MgSO}_4 \cdot 7 \text{H}_2\text{O}$ , 1  $\text{MnSO}_4 \cdot \text{H}_2\text{O}$ , 1  $\text{FeSO}_4 \cdot 7 \text{H}_2\text{O}$ , 1  $\text{CaCl}_2 \cdot 2 \text{H}_2\text{O}$ , and 20 of sucrose fatty acid ester (SFAE).

### Microbial culture

*B. brevis* was cultured at  $37^\circ\text{C}$  on a rotary shaker at  $100 \text{ r min}^{-1}$  for 3 h–6 days. Subsequently, the cells were centrifuged at  $3500g$  for 5 min and washed three times with sterile distilled water before use. The cellular growth phases were determined by the optical density at 600 nm. All experimental procedures were under aerobic conditions.

### Biosorption, degradation, accumulation, and removal of BDE209

The removal and degradation of  $0.5 \text{ mg L}^{-1}$  BDE209 by  $1 \text{ g L}^{-1}$  *B. brevis* were performed in the dark at  $25^\circ\text{C}$  in 20 mL treatment solution shaken at  $100 \text{ r min}^{-1}$ . After treatment, the cells were separated at  $3500g$ . The residual BDE209 in the supernatant was detected to determine the removal efficiencies, and the total BDE209 in the supernatant and cells was used to determine the degradation efficiencies. The controls were run in parallel in flasks with solutions that were not inoculated.

To clarify the trend of BDE209 biosorption, the BDE209-loaded cells were washed by a phosphate-buffered solution (PBS) for 20 min. Subsequently, BDE209 in PBS was analyzed to determine the BDE209 absorbed by the cellular surface and BDE209 in residual cells was detected to determine the BDE209 accumulation. The nutrient use, ion and monosaccharide released by cells, the metabolites of BDE209 degradation, and cellular membrane permeability were also analyzed after degradation for 0–7 days.

The ratios of BDE209 biosorption, degradation, accumulation, and removal are calculated as follows:

$$Q = (C_c - C_t) \times 100 / C_c$$

where  $Q$  represents the ratio (%),  $C_c$  stands for the BDE209 concentration shown in the control experiment, and  $C_f$  is the final concentration of BDE209 after treatment.

### Analyses of BDE209 and its metabolites

Each sample was freeze-dried and then extracted twice, for 30 min each time, with 20 mL of a mixture of *n*-hexane and acetone (1:1, *v/v*) in an ultrasonic bath set at 500 W. The extraction procedure was then repeated using 20 mL of a mixture of *n*-hexane and methylene chloride (1:1, *v/v*). The organic portion was collected, concentrated, and transferred into 10 mL of chromatographic grade *n*-hexane before the extract was analyzed.

The BDE209 metabolites in the extract were analyzed by gas chromatography–mass spectrometry, using the mass spectrometer in negative chemical ionization mode and selected ion-monitoring mode. A DB–XLB capillary column (30 m long, 0.25 mm i.d., 0.25- $\mu\text{m}$  film thickness; Agilent Technologies, Santa Clara, CA, USA) was used to separate the tri- to hepta-bromodiphenyl ether (BDE) congeners (BDEs 28, 47, 66, 138, and 183). The initial oven temperature was 110 °C, which was held for 1 min, then the temperature was increased to 180 °C at 8 °C  $\text{min}^{-1}$  (held for 1 min), then to 240 °C at 2 °C  $\text{min}^{-1}$  (held for 5 min), then to 280 °C at 2 °C  $\text{min}^{-1}$  (held for 25 min), and then to 290 °C at 5 °C  $\text{min}^{-1}$  (held for 13 min). The octa- to deca-BDE congeners (BDEs 196, 197, 203, 206, 207, 208, and 209) were separated using a DB–5HT capillary column (15 m long, 0.25 mm i.d., 0.10- $\mu\text{m}$  film thickness; Agilent Technologies). The initial oven temperature was 110 °C, and the temperature was increased to 300 °C at 8 °C  $\text{min}^{-1}$  (held for 20 min). A 1- $\mu\text{L}$  aliquot of a sample was injected using an autosampler, and the injection port was used in splitless mode. The carrier gas was helium, and the flow rate was 1 mL  $\text{min}^{-1}$ . The chemical ionization moderating gas was methane, and the ion source pressure was  $2.4 \times 10^{-3}$  Pa. The ion source and interface temperatures were 200 and 280 °C, respectively (Tian et al. 2012).

Quantification was achieved using linear calibration curves made using PBDE standard solutions at seven concentrations. The limit of detection was defined as the concentration giving a signal five times (or three times for BDE209) the noise level. Linear regression equations and  $r^2$  values were obtained by plotting the integrated peak area ( $y$ ) against the PBDE concentration ( $x$ ). All of the measured concentrations were within the calibration curve ranges.

### Analyses of ions, organic acids, and arabinose

After the BDE209 degradation tests had been performed, each treated solution was centrifuged at 3500g for 10 min. The supernatant was filtered through a 0.22- $\mu\text{m}$  polyether sulfone

filter, and the  $\text{Cl}^-$ ,  $\text{PO}_4^{3-}$ ,  $\text{SO}_4^{2-}$ ,  $\text{NO}_3^-$ ,  $\text{Na}^+$ ,  $\text{K}^+$ ,  $\text{NH}_4^+$ ,  $\text{Mg}^{2+}$ , arabinose, acetic acid, and oxalic acid concentrations in the solution were determined using an ICS-2500 ion chromatograph system (Dionex, Sunnyvale, CA, USA).

### Analytical methods of intracellular and extracellular proteins

After BDE209 degradation, the cells were separated and the supernatant was used to determine the extracellular protein concentration. Meanwhile, the cells were washed three times in cold PBS (pH 7.4), suspended in a cold lysis buffer (30 mM Tris–HCl, 7 M urea, 2 M thiourea, and 4 % *w/v* CHAPS at pH 8.5), and lysed by sonication in an ice bath for 15 min. The cellular debris was removed from the suspension at 16,000g for 5 min at 4 °C, and the supernatant protein concentration was quantified by the Bradford method.

### Cellular membrane permeability

Membrane permeability was determined by measuring the concentration of  $\beta$ -galactosidase released into the solution using *o*-nitrophenyl- $\beta$ -D-galactoside (ONPG) as a substrate (Shi et al. 2013).

### Cellular activities in carbon nutrient use

After BDE209 degradation, a 1 mL sample was mixed with 99 mL of 0.85 % sterilized NaCl solution. Then, a solution of 150  $\mu\text{L}$  was inoculated into each well of the Biolog microplate and incubated at 25 °C in the dark. The optical density at 590 nm of each well was determined every 12 h.

### Computational methods

The structures of BDE209, peptidoglycan, and cell membrane were drawn in ChemBioDraw Ultra version 13.0 and then copied to ChemBio3D Ultra version 13.0 to create the three-dimensional model. Subsequently, these structures were subjected to energy minimization by molecular mechanics until the root-mean-square gradient became smaller than 0.01 kcal  $\text{mol}^{-1}$  Å. The interaction between BDE209 and cellular compounds was calculated by molecular dynamics. The step interval, frame interval, and terminate of the calculation were 2 fs, 10 fs, and 10,000 steps, respectively. The bond atom, dihedral atom, and angle atom characteristics of these interacted compounds were obtained by compute properties.

### Statistical analysis

All of the experiments were performed in triplicate, and the mean values were used in the calculations. The statistical analysis of the correlation between the BDE209 degradation and

cellular metabolic response was performed using SPSS version 13.0 using Pearson’s correlation tests. The molecular properties of BDE209 and its metabolites were analyzed by ChemBioOffice version 13.

## Results and discussion

### BDE209 biodegradation

The cell density was determined after the cells had been cultured for different times to allow the cellular growth phase at each time point to be determined. A very short lag phase (2–5 h) can be seen in Fig. 1a. This indicated that *B. brevis* adapted to the culture medium quickly. The amount of biomass present increased sharply after the lag phase, peaked at 12 h, and then remained stable. Cells cultured for different times were collected and used to degrade BDE209 to determine the optimal inoculation time for treating BDE209. The degradation curve resembled the growth curve, confirming that the biodegradation of BDE209 through metabolism relies on the activities of the enzymes present. Expressions of the relevant enzymes would have been upregulated when the cells had been cultured for the suitable amount of time, promoting the biodegradation of BDE209.

The BDE209 degradation efficiency increased, and the degradation capacity per gram of cells decreased as the amount of biomass present increased, as is shown in Fig. 1b. The BDE209 degradation efficiency increased primarily because the amounts of enzymes involved in BDE209 degradation increased as the amount of biomass present increased. The degradation capacity decreased because fewer collisions per gram of cells occurred between BDE209 molecules and the cells as the amount of biomass increased and because of fierce competition among the cells for nutrients at high biomass concentrations. A cell concentration of 1 g L<sup>-1</sup> and a cultivation time of 1 day gave a high cell density and the optimal BDE209 degradation efficiency, so these conditions were used in further experiments.

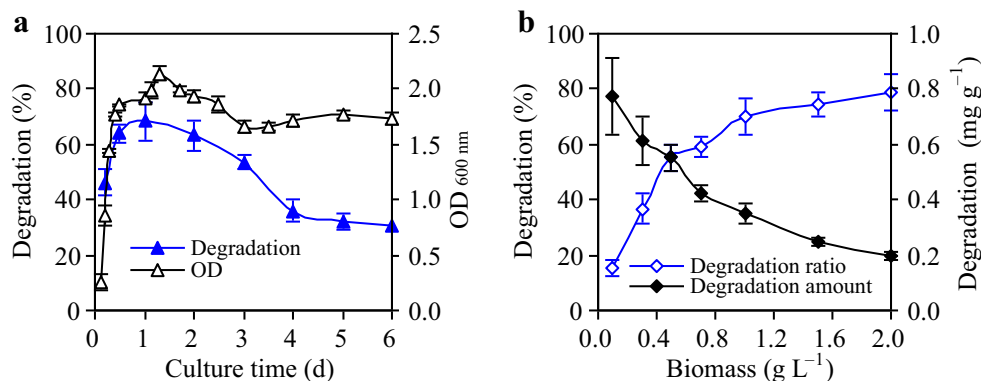
### BDE209 biosorption, biodegradation, and bioaccumulation

The amounts of BDE209 removed, absorbed, degraded, and accumulated were determined by measuring the decrease in the BDE209 concentration in the treated solution, the amount of BDE209 absorbed to the cell surfaces, the decrease in the total BDE209 concentration in the solution and the cells, and the amount of BDE209 found inside the cells, respectively. The amount of BDE209 removed therefore consisted of the amount of BDE209 absorbed to the cell surfaces, the amount transformed through being metabolized in the cells, and the amount accumulated in the cells. The increase in the removal efficiency, from 76.1 to 94.6 %, over days 1–7 of the treatment period was primarily ascribed to the biodegradation rate increasing from 30.2 to 69.5 % over that period (Fig. 2a). The BDE209 inside the cells would have continually been subject to being transformed, but the BDE209 concentration inside the cells remained stable at between 18.7 and 25.7 % for the first 4 days. It can be deduced that a portion of the BDE209 that had been absorbed was continually transported into the cells and degraded, and this was confirmed by the biosorption efficiency decreasing.

As is shown in Fig. 2a, the BDE209 removal process was fast and the degradation, biosorption, and accumulation efficiencies were high, at 30.2, 23.7, and 18.7 %, respectively, on the first treatment day. The degradation rate clearly decreased each day after the first day, and this was probably caused by nutrient deficiencies, the release of intracellular BDE209, the degradation of metabolites, fewer collisions between cells and residual BDE209 occurring, or a combination of these factors. In addition, prolonged exposure to BDE209 and its metabolites negatively influenced metabolic activity in *B. brevis*. PBDEs, because of their toxicological properties, have been found to inhibit various organisms (Dingemans et al. 2007).

SFAE in the treatment medium would emulsify BDE209, improve the solubility of BDE209, and enhance the contact between BDE209 and the cells, resulting in more BDE209

**Fig. 1** Degradation of 0.5 mg L<sup>-1</sup> BDE209 by *B. brevis* at 25 °C for 7 days. **a** Cell density in the culture medium at different culture times and BDE209 degradation in the treatment solution by 1 g L<sup>-1</sup> cells separated at different culture times and **b** BDE209 degradation by cells at 0.1–2 g L<sup>-1</sup>



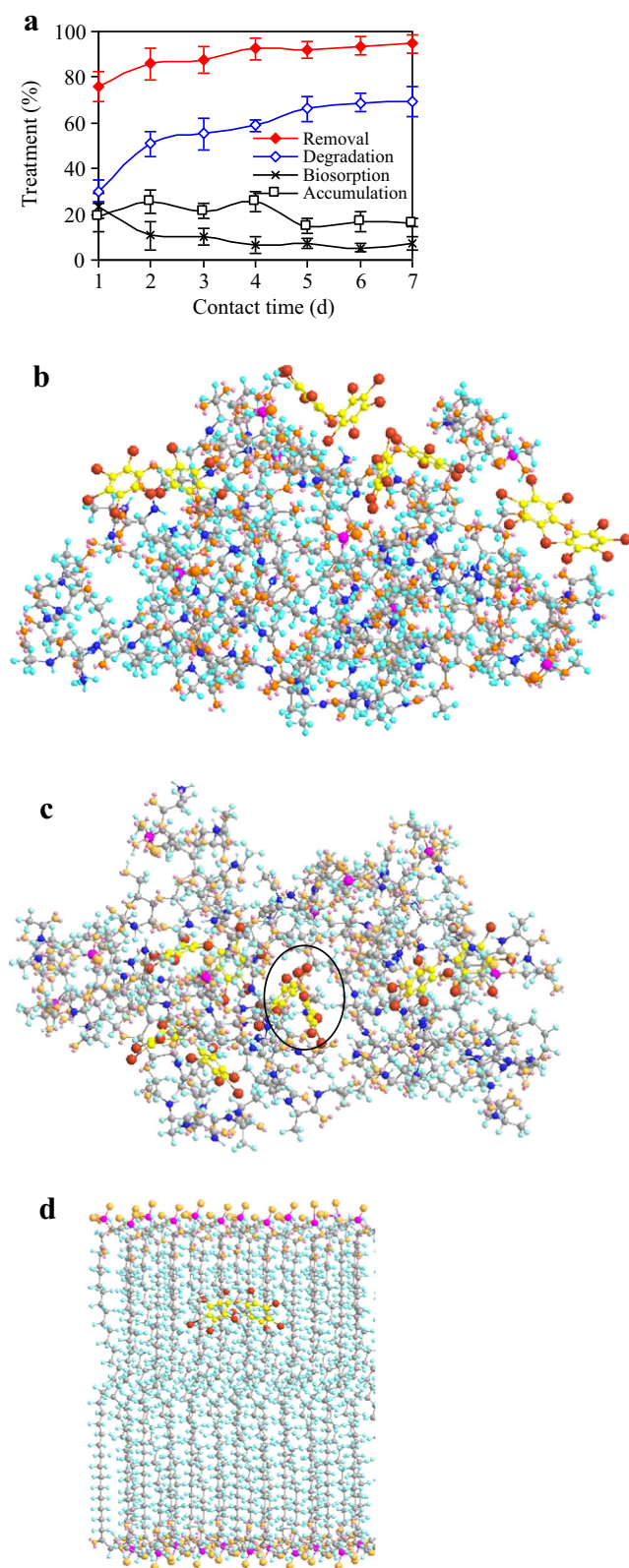


**Fig. 2** BDE209 biosorption, biodegradation, and bioaccumulation. **a** Biosorption, degradation, and accumulation of  $0.5 \text{ mg L}^{-1}$  BDE209 by *B. brevis* at  $25^\circ\text{C}$ ; **b** and **c** BDE209 biosorption by the cell wall; and **d** BDE209 biosorption by the cell membrane

being absorbed by the cells. The dissolved BDE209 tended to be absorbed by the lipophilic components in the cell membranes because of the affinity between BDE209 and such components. The uptake of dissolved BDE209 into the cytoplasm through diffusion and active transport would have been increased partly because of the increase in the solubility of BDE209 and the increased amount of BDE209 absorbed, caused by the presence of the sucrose fatty acid esters. This then increased the amount of degraded BDE209 because the degradation process took place within the cells. Being a biodegradable surfactant produced through esterification or acylation reactions between fatty acids and sucrose, the SFAE in the treatment solution would have served as a nutrient for cellular metabolism and been partly responsible for the increased degradation of BDE209 that was found.

The maximum biosorption was found after 1 day, showing that the BDE209 binding process occurred quickly. This would have been because BDE209 is hydrophobic, so it tends to bond with the major cell wall and membrane components (Ye et al. 2013b). As is shown in Fig. 2b, the BDE209 initially tended to be absorbed by the wall teichoic acid and the  $-\text{N}(\text{H})-\text{C}(\text{O})-\text{CH}_3$  side chains in peptidoglycan. The wall teichoic acid, being the outer layer of the cell, is an important route through which bacteria obtain nutrients. Teichoic acid can take on topological structures suitable for adsorbates with various structures because it has a long chain and contains a range of units. The teichoic acid polymers in the cell walls chelated BDE209 by changing their topological structures, and their hydrophobic chains caused BDE209 to be absorbed. The absorbed BDE209 subsequently altered the topological structures of the peptide chains, then created pores within the peptidoglycans (Fig. 2c), accelerating BDE209 transport through the cell walls. Peptidoglycans consist of alternating N-acetylglucosamine and N-acetylmuramic acid residues connected by  $\beta$ -(1–4)-glycosidic bonds. The cell wall polymer is formed because a pentapeptide in each N-acetylmuramic acid is linked to another glycan chain (Kim et al. 2014). These cell wall polymers contain pores 30 to 70 Å in diameter, which easily allowed BDE209 to pass through the polymers (Fig. 2c).

PBDEs are highly lipophilic and tend to accumulate in the lipids of organisms. Ignoring the possibility of active transport, sorption accelerated by attraction between BDE209, and the hydrophobic tails in cell membranes (containing molecules with carbon chain lengths of 14–22) contributed to BDE209 diffusion through the cell membrane or BDE209 accumulation in the membrane (Fig. 2d). Up to 29.6 % of PBDEs in the air cells have been found to be absorbed into the eggs, showing that PBDEs can diffuse through cell membranes (McKernan et al. 2010). After being absorbed to a cell membrane, BDE209 was transported to within the cell and degraded by enzymes.

### BDE209 transformation and the molecular properties of the metabolites

The concentrations of the BDE209 debromination products decreased in the order of nona-BDEs, octa-BDEs, and hepta-BDEs. The nona-BDE concentrations were approximately 31–63  $\mu\text{g L}^{-1}$  (Fig. 3a). The octa-BDE concentrations were approximately 3–11  $\mu\text{g L}^{-1}$  (Fig. 3b), and the hepta-BDE concentrations were lower, as shown in Fig. 3c. The BDE47 (6.4–18.6  $\text{ng L}^{-1}$ ) and BDE28 concentrations (1.7–6.4  $\text{ng L}^{-1}$ ) were much lower (Fig. 3d). These results confirmed that BDE209 was degraded through three debromination pathways (Fig. 3f). The pathways were BDE209→BDE206→BDE203→BDE183→BDE138→BDE47→BDE28, BDE209→BDE207→BDE196/BDE197→BDE66→BDE28, and BDE209→BDE208. The metabolites listed above have been found in various samples, showing that BDE209 is transformed in the environment, organisms, and humans through similar pathways to those found in this study (Chua et al. 2014; Lohmann et al. 2013; Yu et al. 2011). Although BDE209 degradation by *B. brevis* primarily occurs through debromination, the total PBDE concentration decreased with time, as shown in Fig. 3e, indicating that some of the BDE209 was transformed into diphenyl ether and other metabolites that did not contain bromine.

The molecular properties of BDE209 and its metabolites, calculated using ChemBioOffice, showed that the C(1)–Br and C(9)–Br bonds are the easiest to cleave because they are the lowest-energy bonds (0.257  $\text{kcal mol}^{-1}$ ; Table S1) and have the lowest atom angle energies (0.001  $\text{kcal mol}^{-1}$ ; Table S2) of all of the C–Br and C–C–Br bonds. This explains why BDE206 was the main degradation product and had a higher concentration than the other products in the current study. Apart from the lowest atom angle energy for C(11)–C(12)–Br in BDE206, more orbital electrons were found to be attracted by the bromine atom linked to C(12) (Fig. S1), which was indicated by the highest occupied molecular orbital (HOMO) of BDE206. This would have meant that the C(12)–Br bond in BDE206 would have broken to give BDE203.

The C–Br bond energies showed that the more brominated PBDEs are less reactive than the less brominated PBDEs. The C–C bond energies were found to decrease as fewer bromine atoms are linked to the diphenyl groups, suggesting that diphenyl ether will be less toxic and more degradable than the PBDEs (Table S1). The molecular properties (including the boiling points, melting points, critical temperatures, critical pressures, critical volumes, Gibbs energies, heats of formation, LogP values, CLogP values, and Henry's constants) of the metabolites are shown in Table S3. These properties confirmed that the more bromine atoms there are in a PBDE, the slower the PBDE will be transformed. The molecular

**Fig. 3** Biodegradation metabolites of 0.5  $\text{mg L}^{-1}$  BDE209 by *B. brevis* at 25 °C. **a** Concentrations of BDE208, BDE207, and BDE206; **b** concentrations of BDE203, BDE197, and BDE196; **c** concentrations of BDE183, BDE138, and BDE66; **d** concentrations of BDE47 and BDE28; **e** concentrations of the residual BDE209, total metabolites, and PBDEs; and **f** three debromination pathways of BDE209 degradation

energy data, especially the stretch energies and bend energies, which are shown in Table S4, also supported this conclusion. This means that BDE47 and BDE28 will be transformed quickly, resulting in them being found at low concentrations. BDE28 was found at significantly lower concentrations than its parent PBDEs, BDE66 and BDE47, which further confirmed the conclusions given above.

The rapid elimination of BDE47 has been found in kestrels even though BDE47 is one of the most environmentally abundant, toxic, and bioaccumulative of the PBDE congeners and has been found to magnify in most aquatic food webs that have been studied (Yu et al. 2011). The current study also found that BDE47 was quickly transformed, and this shows that BDE209 degradation by *B. brevis* is an environmentally beneficial process, especially compared with debromination, which has previously been found only to decrease BDE47 concentrations by 30 % after 8 months of incubation (Tokarz et al. 2008). Although the analytical methods of PBDEs could detect low brominated congeners even di-BDEs (Tian et al. 2012), bromide PBDEs lower than BDE28 were not detected in the current study. This further verified that *B. brevis* transformed the less brominated congeners more quickly than the more brominated congeners and that BDE209 was degraded efficiently by *B. brevis* under the experimental conditions.

The energy gap between the HOMO and the lowest unoccupied molecular orbital (LUMO) for each of the PBDEs was found to be significantly lower than the gap for benzene (see Table S5 and Fig. S1). More energy would be needed for an electron in the HOMO of benzene than for an electron in the HOMO of a PBDE to jump into the LUMO and bring the molecule into an excited electronic state. This explains why BDE209 will initially tend to be debrominated rather than one of the benzene rings breaking.

### Changes in membrane permeability and cellular nutrient use activities during BDE209 removal

Extracellular ONPG can be transported into a cell and hydrolyzed to give *o*-nitrophenol when membrane permeability increases (Shi et al. 2013). The appearance of *o*-nitrophenol in a solution indicates that  $\beta$ -galactosidase has induced the hydrolysis of the ONPG that has entered cells. The increasing optical density at 405 nm (Fig. 4a) indicated that the cell membrane permeability tended to alter over time. The high optical density of the solution treated with BDE209 confirmed that adding BDE209, which was associated with the increased

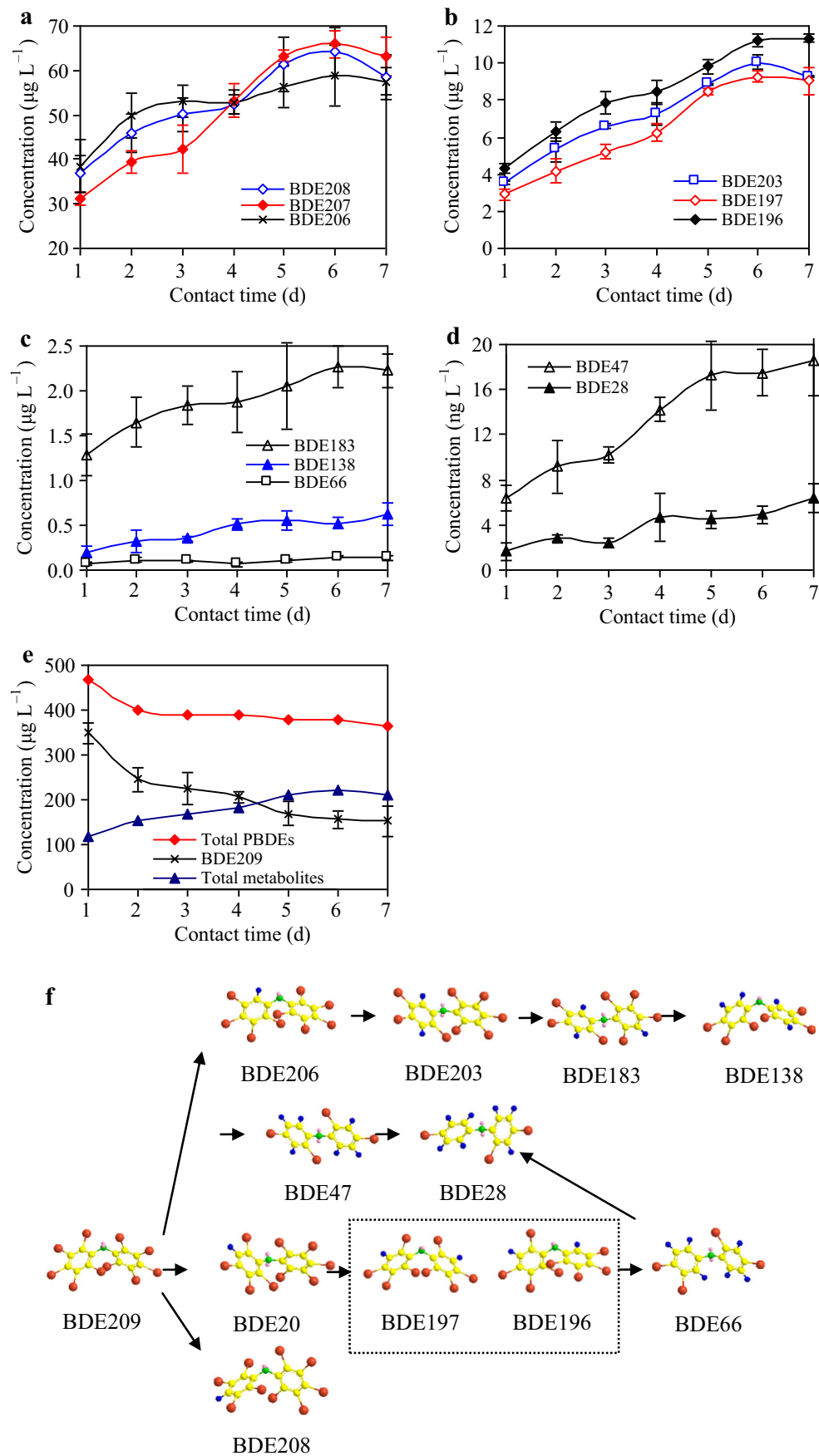
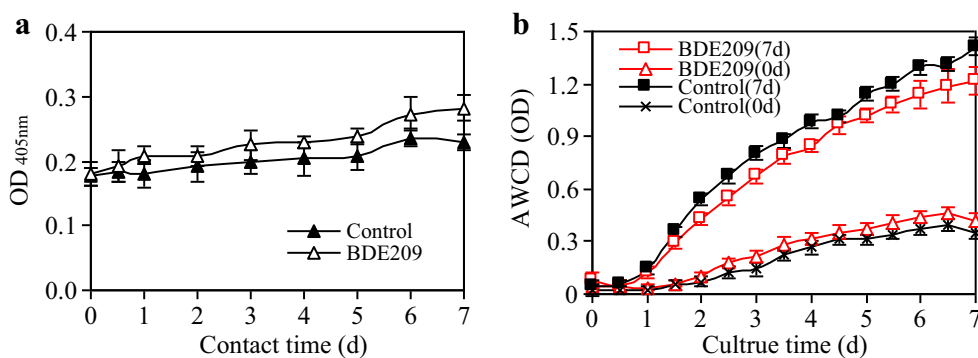


**Fig. 4** Membrane permeability change and cellular nutrient use activities during BDE209 removal. **a** Membrane permeability change in the control cells and BDE209-treated cells with contact time and **b** nutrient use activities of cells at different times before and after BDE209 degradation

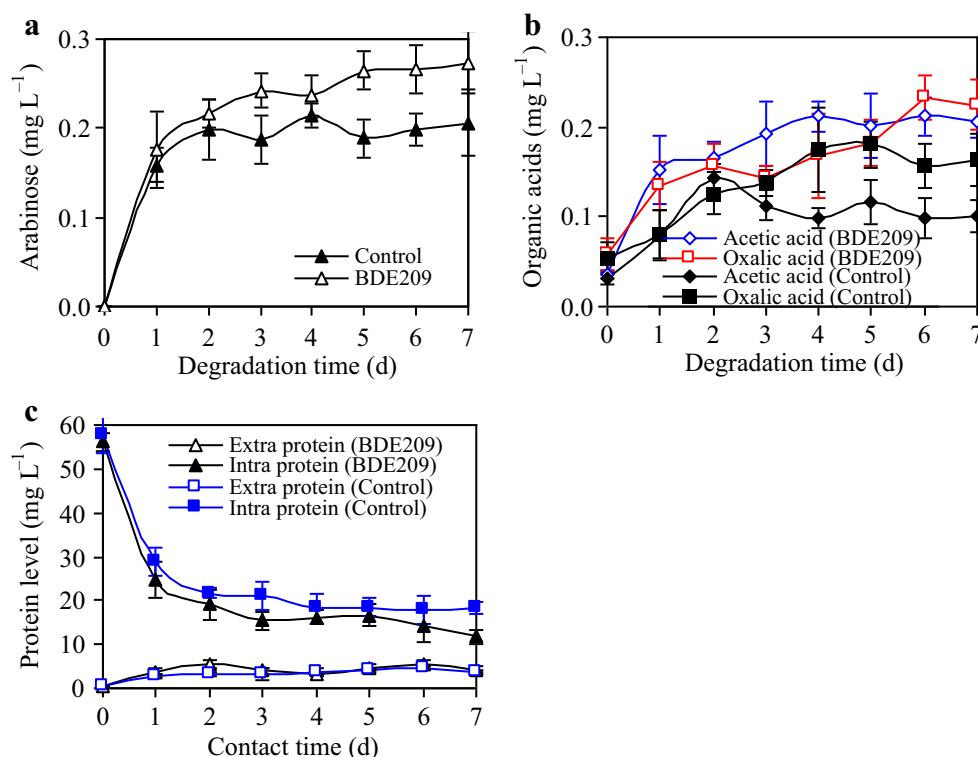


release of arabinose, organic acids, proteins (Fig. 5), and ions (Fig. 6), caused the membrane permeability to increase significantly because of oxidative stress in the membrane (Calabrese et al. 2010). The change in the membrane permeability would have been one of the reasons BDE209 was desorbed or released into the solution (Fig. 2d), and this would have been part of the reason the BDE209 removal and degradation efficiencies increased slowly over time. The optical densities of the control samples also increased over time but significantly less than the optical densities of the BDE209-treated samples (Fig. 4a), and this would have been because the control samples were deficient in exotic carbon-containing nutrients.

The nutrient use activity of the cells was slightly higher for the cells treated with BDE209 for 0 day than for the controls (Fig. 4b), and this was primarily the result of amino acids

being increasingly used in the BDE209-treated cells (Fig. S2). This would have been a result of specific proteins being synthesized to resist the toxicity of BDE209. However, the nutrient use activity in the cells that were treated for 7 days increased dramatically because of the germination of abundant bacterial spores. Being a *Bacillus* species, *B. brevis* tends to form endospores in response to starvation or stress caused by pollutants. Some of the cells will have formed endospores after being inoculated in the treatment solution for 7 days, and these endospores would have germinated in Biolog plates. Abundant organic carbon has been found to be needed when spores germinate on Biolog plates, and this was found to increase the rate at which extracellular nutrients were assimilated (Brar et al. 2007). The cells treated with BDE209 for 7 days generally used less nutrients than did the control samples, and this would have been because BDE209 acted as a carbon

**Fig. 5** Arabinose, organic acid, and protein release by cells during BDE209 removal. **a** Arabinose release, **b** organic acid release, and **c** protein release and change in the intracellular protein concentration



source. Specifically, the cells treated with BDE209 for 7 days used more carbohydrates but less alcohols, amines, carboxylic acids, and esters than did the cells in the control samples, as is shown in Fig. S2.

### Release of arabinose, organic acids, and proteins by cells during BDE209 removal

Arabinose, organic acids, and proteins were not added to the test solutions, so the presence of these compounds in the solutions indicated that they had been produced by the cells. The arabinose concentration increased quickly on the first day of the tests and rose slowly subsequently (Fig. 5a). More arabinose was produced in the BDE209-treated samples than in the control samples. Monosaccharides are easily ingested by cells unless the cells are damaged in some way. Therefore, the increasing arabinose concentration indicated that the presence of PBDEs and a nutrient deficiency affected the cell membranes and caused certain intracellular monosaccharides to be driven out of the cells or inhibited the reuse of the monosaccharides. Arabinose has been found to be transported through the pentose phosphate pathway (Wisselink et al. 2010). This pathway can be inhibited by a nutrient deficiency and by pollutant stress, causing arabinose to be released. The release of arabinose will slow, and cells will start to take up arabinose when a certain extracellular arabinose concentration is reached, which is controlled by *GAL* regulon (Upadhyay and Sasidhar 2012). The slow increases in the arabinose concentrations after 1 day had passed in the current tests and therefore illustrated that cell activity was not severely inhibited. Furthermore, no other monosaccharides were detected, demonstrating that BDE209 did not induce serious damage or apoptosis (which would have caused the obvious production of other cytosolic monosaccharides) in most of the *B. brevis* cells.

More organic acids were produced by the cells exposed to BDE209 than in the cells in the control samples (Fig. 5b). Apart from the membrane permeability increasing, this could have been caused by the functional poly(3-hydroxybutyrate) (PHB) homopolymer synthetic pathway being damaged. This pathway warrants that a microorganism produces PHB and survives better under adverse conditions. The inhibition of the pathway has been found to lead to metabolic turmoil, such as the overproduction of organic acids, including acetate, citrate, glutamate, lactate, and pyruvate (Chen et al. 2012). The phosphorylated enzymes  $\alpha$ -dehydro- $\beta$ -deoxy-D-glucarate aldolase, phosphoenol pyruvate synthetase, and enolase have also been found to be involved to significant degrees, along with isocitrate dehydrogenase, in regulating acetate metabolism. Protein phosphorylation is important to the transport of carbonaceous organic materials (Lim et al. 2015).

The intracellular protein concentrations decreased quickly on the first day of the tests and decreased slowly thereafter

(Fig. 5c). The extracellular protein concentrations were almost the same in the BDE209-treated cells and the cells in the control samples. The intracellular protein concentrations in the BDE209-treated samples decreased over time, and this would have been related to protein degradation and release, caused by pollutant stress, and the membrane permeability increasing (Fig. 4a). These conclusions were partly verified by the extracellular protein concentration increasing relative to the concentration at the beginning of the experiment. The decreases in the amount of biomass present and the intracellular protein concentrations that were found, and the suppressed metabolic activity of *B. brevis* that followed, would have been caused by the toxicity of BDE209 or a lack of sources of carbon. PBDEs have been reported to alter the structures of proteins and to degrade some proteins, such as post-synaptic proteins in mice (Dingemans et al. 2007). The slow decreases in the intracellular protein concentrations during the late stages of the degradation process were consistent with the decreases found in the residual BDE209 concentrations in the solutions but could have been caused by the protein concentration gradient decreasing.

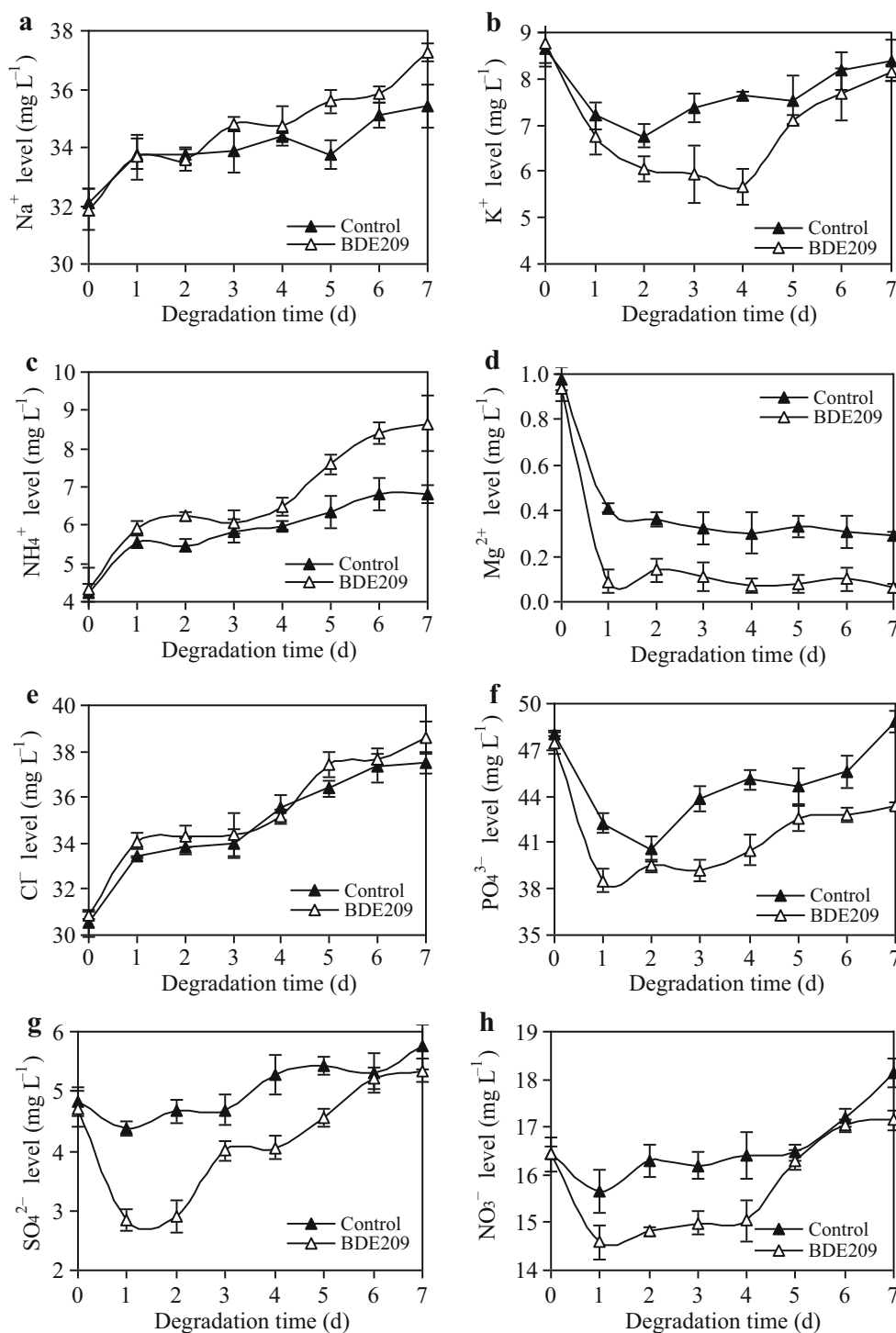
### Metabolism of ions by the cells during BDE209 removal

As is shown in Fig. 6,  $\text{Na}^+$ ,  $\text{NH}_4^+$ , and  $\text{Cl}^-$  were released throughout the whole degradation process. The increased release of ions by cells exposed to BDE209 further confirmed that the presence of PBDEs caused the membrane permeability to increase (Fig. 4a) or induced apoptosis (Madia et al. 2004) in some cells. However,  $\text{K}^+$ ,  $\text{Mg}^{2+}$ ,  $\text{PO}_4^{3-}$ ,  $\text{SO}_4^{2-}$ , and  $\text{NO}_3^-$  were assimilated by the cells after BDE209 had been degraded, indicating that stress caused by the presence of PBDEs did not cause serious damage to most of the cells. These findings show that the detrimental effects caused by nutrient deficiencies in the treatment solutions were more serious than the detrimental effects caused by the PBDEs.

The cells were cultured in media containing  $5 \text{ g L}^{-1}$  NaCl, and  $\text{Na}^+$  and  $\text{Cl}^-$  in the cytoplasm of the cells were the sources of the  $\text{Na}^+$  and  $\text{Cl}^-$  released from the cells (Fig. 6e). The metabolism of  $\text{Cl}^-$  mainly depends on the  $\text{Cl}^-$  concentration gradient, which regulates the cellular osmotic pressure (Zhao et al. 2009). Except for stress caused by the presence of PBDEs, the osmotic pressure of the cytoplasm was always higher than the osmotic pressure of the solution. More  $\text{Cl}^-$  was therefore released during the BDE209 removal process.

Changes in the  $\text{Na}^+$  concentrations (Fig. 6a) were jointly caused by pollutant stress, changes in osmotic pressure, and  $\text{Na}^+/\text{K}^+$ -ATPase activities.  $\text{Na}^+/\text{K}^+$ -ATPase is stimulated by binding to extracellular  $\text{K}^+$  and intracellular  $\text{Na}^+$ , and the  $\text{Na}^+/\text{K}^+$ -ATPase transports  $\text{K}^+$  into cells and  $\text{Na}^+$  out of cells. BDE209 could have been actively transported by being co-transported with the  $\text{K}^+/\text{Na}^+$ -ATPase, and this was confirmed by BDE209 being effectively degraded and accumulated on

**Fig. 6** Ion metabolism by *B. brevis* at 25 °C during BDE209 removal. **a** Na<sup>+</sup>, **b** K<sup>+</sup>, **c** NH<sub>4</sub><sup>+</sup>, **d** Mg<sup>2+</sup>, **e** Cl<sup>-</sup>, **f** PO<sub>4</sub><sup>3-</sup>, **g** SO<sub>4</sub><sup>2-</sup>, and **h** NO<sub>3</sub><sup>-</sup>



the first day (Fig. 2). This caused Na<sup>+</sup> to be released but K<sup>+</sup> to be assimilated (Fig. 6b). The K<sup>+</sup> influx decreased significantly after 4 days, and this was consistent with the amount of BDE209 degraded slowly increasing at the same time (Fig. 2a). The transport of Na<sup>+</sup> and K<sup>+</sup> in the opposite direction by Na<sup>+</sup>/K<sup>+</sup>-ATPase did not agree with this sudden change. However, an increase in the release of intracellular material caused by an increase in membrane permeability could

explain the abrupt increases in Na<sup>+</sup> and K<sup>+</sup> transport. The NO<sub>3</sub><sup>-</sup> concentration also increased at the same time (Fig. 6h), and this partly supported our conclusions.

Some biomolecules have NH<sub>4</sub><sup>+</sup> as a component. For example, proteins and peptidoglycans have N-terminal tails. NH<sub>4</sub><sup>+</sup> can therefore be released into solution when such a biomolecule is degraded and the membrane permeability is increased. The NH<sub>4</sub><sup>+</sup> concentrations in the current tests increased

**Table 1** Correlation between BDE209 removal and cellular response

Indexes	Time	Degradation	Removal	Permeability	Intracellular protein	Extracellular protein	Cl <sup>-</sup>	PO <sub>4</sub> <sup>3-</sup>	SO <sub>4</sub> <sup>2-</sup>	NO <sub>3</sub> <sup>-</sup>	Na <sup>+</sup>	K <sup>+</sup>	NH <sub>4</sub> <sup>+</sup>	Mg <sup>2+</sup>	Arabinose	Acetic acid	Oxalic acid	
Time	1																	
Degradation	0.890 <sup>a</sup>	1																
Removal	0.705	0.928 <sup>a</sup>	1															
Permeability	0.969 <sup>a</sup>	0.847 <sup>a</sup>	0.701	1														
Intracellular protein	-0.749 <sup>b</sup>	-0.948 <sup>a</sup>	-0.993 <sup>a</sup>	-0.749 <sup>b</sup>	1													
Extracellular protein	0.589	0.814 <sup>b</sup>	0.869 <sup>a</sup>	0.629	-0.857 <sup>a</sup>	1												
Cl <sup>-</sup>	0.957 <sup>a</sup>	0.910 <sup>a</sup>	0.801 <sup>b</sup>	0.945 <sup>a</sup>	-0.823 <sup>b</sup>	0.730 <sup>b</sup>	1											
PO <sub>4</sub> <sup>3-</sup>	0.032	-0.373	-0.675	-0.023	0.631	-0.578	-0.134	1										
SO <sub>4</sub> <sup>2-</sup>	0.657	0.287	-0.051	0.620	-0.024	-0.102	0.474	0.718 <sup>b</sup>	1									
NO <sub>3</sub> <sup>-</sup>	0.606	0.218	-0.106	0.594	0.045	-0.008	0.490	0.772 <sup>b</sup>	0.931 <sup>a</sup>	1								
Na <sup>+</sup>	0.967 <sup>a</sup>	0.898 <sup>a</sup>	0.780 <sup>b</sup>	0.962 <sup>a</sup>	-0.824 <sup>b</sup>	0.628	0.964 <sup>a</sup>	-0.133	0.535	0.478	1							
K <sup>+</sup>	0.081	-0.349	-0.574	0.125	0.531	-0.391	0.011	0.872 <sup>a</sup>	0.657	0.812 <sup>b</sup>	-0.004	1						
NH <sub>4</sub> <sup>+</sup>	0.960 <sup>a</sup>	0.887 <sup>a</sup>	0.761 <sup>b</sup>	0.968 <sup>a</sup>	-0.789 <sup>b</sup>	0.737 <sup>b</sup>	0.990 <sup>a</sup>	-0.078	0.518	0.552	0.949 <sup>a</sup>	0.079	1					
Mg <sup>2+</sup>	-0.614	-0.857 <sup>a</sup>	-0.985 <sup>a</sup>	-0.630	0.968 <sup>a</sup>	-0.842 <sup>a</sup>	-0.745 <sup>b</sup>	0.756 <sup>b</sup>	0.165	0.209	-0.723	0.606	-0.695	1				
Arabinose	0.810 <sup>b</sup>	0.977 <sup>a</sup>	0.981 <sup>a</sup>	0.793 <sup>b</sup>	-0.990 <sup>a</sup>	0.858 <sup>a</sup>	0.876 <sup>a</sup>	-0.540	0.124	0.062	0.866 <sup>a</sup>	-0.454	0.842 <sup>a</sup>	-0.942 <sup>a</sup>	1			
Acetic acid	0.796 <sup>b</sup>	0.963 <sup>a</sup>	0.978 <sup>a</sup>	0.777 <sup>b</sup>	-0.982 <sup>a</sup>	0.800 <sup>b</sup>	0.845 <sup>a</sup>	-0.558	0.119	0.017	0.843 <sup>a</sup>	-0.507	0.807	-0.943 <sup>a</sup>	0.985 <sup>a</sup>	1		
Oxalic acid	0.930 <sup>a</sup>	0.927 <sup>a</sup>	0.842 <sup>a</sup>	0.949 <sup>a</sup>	-0.862 <sup>a</sup>	0.814 <sup>b</sup>	0.964 <sup>a</sup>	-0.222	0.401	0.416	0.921 <sup>a</sup>	-0.083	0.979 <sup>a</sup>	-0.778 <sup>b</sup>	0.895 <sup>a</sup>	0.877 <sup>a</sup>	1	

<sup>a</sup>Correlation is significant at the 0.01 level (two-tailed)<sup>b</sup>Correlation is significant at the 0.05 level (two-tailed)

(Fig. 6c), and the intracellular protein concentrations decreased (Fig. 5c). This provided further confirmation that protein degradation was partly responsible for the release of  $\text{NH}_4^+$ . The stress caused by the presence of BDE209 accelerated the degradation of proteins significantly, so more  $\text{NH}_4^+$  was released by the cells exposed to BDE209 than by the cells in the control samples.

The  $\text{Mg}^{2+}$  concentrations clearly decreased in the first day of the tests (Fig. 6d), and this would have been related to the functions of  $\text{Mg}^{2+}$  in cells.  $\text{Mg}^{2+}$  is essential to the structural stabilities of nucleotides, the activities of enzymes, and the regulation of metabolism (Romani 2007; Zorbas et al. 2010).  $\text{Mg}^{2+}$  not only activates various enzymes but is also co-transported with various other ions. A great deal of  $\text{Mg}^{2+}$  was therefore assimilated when BDE209 was transported, degraded, and accumulated efficiently at the beginning of the tests (Fig. 2a). The largest amount of  $\text{PO}_4^{3-}$  was assimilated on the first day of the tests, and then  $\text{PO}_4^{3-}$  continually decreased (Fig. 6f). Not only did the transport and degradation of BDE209 during the treatment process require energy but also metabolism (which is dependent on the energy conversion pathways) within the cells needed. These conclusions were drawn from the amounts of  $\text{PO}_4^{3-}$  consumed by the BDE209-treated cells and by the cells in the control samples.

Sulfur is an essential element to organisms. Sulfur is not only an important structural constituent in various proteins and other biomolecules (Matias et al. 2005) but also has specific metabolic functions. As is shown in Fig. 6g, the  $\text{SO}_4^{2-}$  in the control samples was initially assimilated, but then, a significant amount was released on day 4. This would have occurred because of sulfur-containing molecules being degraded because the cells had suffered prolonged starvation. The degradation of BDE209 increased the amount of  $\text{SO}_4^{2-}$  that was assimilated and decreased the amount that was subsequently released. This suggests that the presence of PBDEs inhibited  $\text{SO}_4^{2-}$  metabolism less than did prolonged starvation.

### Correlation between BDE209 removal and cellular metabolism

There were significant relationships between the BDE209 treatment time and the release of  $\text{Cl}^-$ ,  $\text{Na}^+$ ,  $\text{NH}_4^+$ , arabinose, acetic acid, and oxalic acid (Table 1), and these relationships were consistent with membrane permeability increasing. A significant correlation was found between the removal and degradation of BDE209, showing that BDE209 removal was primarily dependent on BDE209 being degraded. Furthermore, both BDE degradation and removal correlated significantly with the release of  $\text{Cl}^-$ ,  $\text{Na}^+$ ,  $\text{NH}_4^+$ , arabinose, organic acids, and protein; the uptake of  $\text{Mg}^{2+}$ ; and decreasing intracellular protein concentrations. These correlations show that exposure to BDE209 and the transformation of BDE209 suppressed cellular metabolism. However, PBDEs did not

severely damage most of the cells because the PBDE concentrations continued to decrease with time, BDE209 continued to be degraded, the intracellular protein concentration remained relatively high throughout the process, and some of the ions were continually assimilated by the cells.

### Conclusions

The wall teichoic acid and the N-acetylglucosamine side chains in the peptidoglycan of *B. brevis* initially absorbed BDE209, and the BDE209 was subsequently transported into the cells and degraded. BDE209 was degraded through three debromination pathways, and tri-, hepta-, octa-, and nona-BDE congeners were produced. The C(1)–Br and C(9)–Br bonds were found to be easiest to cleave, and the C–C bond energy decreased as the number of bromine atoms linked to the diphenyl backbone decreased. The presence of PBDEs inhibited protein expression; increased membrane permeability; and increased the amounts of  $\text{Cl}^-$ ,  $\text{Na}^+$ ,  $\text{NH}_4^+$ , arabinose, protein, acetic acid, and oxalic acid released. However, the presence of PBDEs increased the amounts of  $\text{K}^+$ ,  $\text{Mg}^{2+}$ ,  $\text{PO}_4^{3-}$ ,  $\text{SO}_4^{2-}$ , and  $\text{NO}_3^-$  that were assimilated.

**Acknowledgments** The authors would like to thank the National Natural Science Foundation of China (Nos. 21377047 and 21577049), Science and Technology Project of Guangdong Province (No. 2014A020216013), and the University Foundation of Education Ministry of China (No. 21615459) for their financial support.

### References

- Brar SK, Verma M, Tyagi RD, Surampalli RY, Barnabé S, Valéro JR (2007) *Bacillus thuringiensis* proteases: production and role in growth, sporulation and synergism. *Process Biochem* 42:773–790
- Calabrese V, Cornelius C, Dinkova-Kostova AT, Calabrese EJ, Mattson MP (2010) Cellular stress responses, the hormesis paradigm, and vitagenes: novel targets for therapeutic intervention in neurodegenerative disorders. *Antioxid Redox Sign* 13:1763–1811
- Chen DJ, Xu D, Li MS, He J, Gong YH, Wu DD, Sun M, Yu ZN (2012) Proteomic analysis of *Bacillus thuringiensis*  $\Delta\text{phaC}$  mutant BMB171/PHB-1 reveals that the PHB synthetic pathway warrants normal carbon metabolism. *J Proteomics* 75:5176–5188
- Chua EM, Shimeta J, Nugegoda D, Morrison PD, Clarke BO (2014) Assimilation of polybrominated diphenyl ethers from microplastics by the marine amphipod, *Allorchestes compressa*. *Environ Sci Technol* 48:8127–8134
- Dingemans MML, Ramakers GMJ, Gardoni F, van-Kleef GDM, Bergman A, DiLuca M, van-den-Berg M, Westerink RHS, Vijverberg HPM (2007) Neonatal exposure to brominated flame retardants BDE-47 reduces long-term potentiation and postsynaptic protein levels in mouse hippocampus. *Environ Health Persp* 115: 865–870
- Guardia MJL, Hale RC, Harvey E, Mainor TM, Ciparis S (2012) In situ accumulation of HBCD, PBDEs, and several alternative flame-retardants in the bivalve (*Corbicula fluminea*) and gastropod (*Elimia proxima*). *Environ Sci Technol* 46:5798–5805

- He J, Robrock KR, Alvarez-Cohen L (2006) Microbial reductive debromination of polybrominated diphenyl ethers (PBDEs). *Environ Sci Technol* 40:4429–4434
- Johansson AK, Sellstrom U, Lindberg P, Bignert A, Cynthia ADW (2011) Temporal trends of polybrominated diphenyl ethers and hexabromocyclododecane in Swedish peregrine falcon (*Falco peregrinus*) eggs. *Environ Int* 37:678–686
- Kim MN, Yoon MG (2010) Isolation of strains degrading poly(vinyl alcohol) at high temperatures and their biodegradation ability. *Polym Degrad Stab* 95:89–93
- Kim SJ, Chang J, Singh M (2014) Peptidoglycan architecture of Gram-positive bacteria by solid-state NMR. *Biochim Biophys Acta* 1848:350–362
- Lee LK, Ding C, Yang KL, He JZ (2011) Complete debromination of tetra- and penta-brominated diphenyl ethers by a coculture consisting of *Dehalococcoides* and *Desulfovibrio* species. *Environ Sci Technol* 45:8475–8482
- Lim S, Marcellin E, Jacob S, Nielsen LK (2015) Global dynamics of *Escherichia coli* phosphoproteome in central carbon metabolism under changing culture conditions. *J Proteomics* 126:24–33
- Lohmann R, Klanova J, Kukucka P, Yonis S, Bollinger K (2013) Concentrations, fluxes, and residence time of PBDEs across the tropical Atlantic Ocean. *Environ Sci Technol* 47:13967–13975
- Madia F, Giordano G, Fattori V, Vitalone A, Branchi I, Capone F, Costa LG (2004) Differential in vitro neurotoxicity of the flame retardant PBDE-99 and of the PCB Aroclor 1254 in human astrocytoma cells. *Toxicol Lett* 154:11–21
- Matias PM, Pereira IAC, Soares CM, Carrondo MA (2005) Sulphate respiration from hydrogen in *Desulfovibrio* bacteria: a structural biology overview. *Prog Biophys Mol Bio* 89:292–329
- McKernan MA, Rattner BA, Hatfield JS, Hale RC, Ottinger MA (2010) Absorption and biotransformation of polybrominated diphenyl ethers DE-71 and DE-79 in chicken (*Gallus gallus*), mallard (*Anas platyrhynchos*), American kestrel (*Falco sparverius*) and black-crowned night-heron (*Nycticorax nycticorax*) eggs. *Chemosphere* 79:100–109
- Qiu MD, Chen XJ, Deng DY, Guo J, Sun GP, Mai BX, Xu MY (2012) Effects of electron donors on anaerobic microbial debromination of polybrominated diphenyl ethers (PBDEs). *Biodegradation* 23:351–361
- Rayne S, Ikonou MG, Whale MD (2003) Anaerobic microbial and photochemical degradation of 4,4'-dibromodiphenyl ether. *Water Res* 37:551–560
- Robrock KR, Korytar P, Alvarez-Cohen L (2008) Pathways for the anaerobic microbial debromination of polybrominated diphenyl ethers. *Environ Sci Technol* 42:2845–2852
- Romani A (2007) Regulation of magnesium homeostasis and transport in mammalian cells. *Arch Biochem Biophys* 458:90–102
- Shi GY, Yin H, Ye JS, Peng H, Li J, Luo CL (2013) Effect of cadmium ion on biodegradation of decabromodiphenyl ether (BDE-209) by *Pseudomonas aeruginosa*. *J Hazard Mater* 263:711–717
- Sulimma L, Bullach A, Kusari S, Lamshoft M, Zuhlke S, Spittler M (2013) Enantioselective degradation of the chiral fungicides metalaxyl and furalaxyl by *Brevibacillus brevis*. *Chirality* 25:336–340
- Tang SY, Bai JQ, Yin H, Ye JS, Peng H, Liu ZH, Dang Z (2014) Tea saponin enhanced biodegradation of decabromodiphenyl ether by *Brevibacillus brevis*. *Chemosphere* 114:255–261
- Tian M, Chen SJ, Wang J, Luo Y, Luo XJ, Mai BX (2012) Plant uptake of atmospheric brominated flame retardants at an E-waste site in southern China. *Environ Sci Technol* 46:2708–2714
- Tokarz JA, Ahn MY, Leng J, Filley TR, Nies L (2008) Reductive debromination of polybrominated diphenyl ethers in anaerobic sediment and a biomimetic system. *Environ Sci Technol* 42:1157–1164
- Upadhyay SK, Sasidhar YU (2012) Molecular simulation and docking studies of Gal1p and Gal3p proteins in the presence and absence of ligands ATP and galactose: implication for transcriptional activation of GAL genes. *J Comput Aid Mol Des* 26:847–864
- Wisselink HW, Cipollina C, Oud B, Crimi B, Heijnen JJ, Pronk JT, van Maris AJA (2010) Metabolome, transcriptome and metabolic flux analysis of arabinose fermentation by engineered *Saccharomyces cerevisiae*. *Metab Eng* 12:537–551
- Xu GY, Wang JB (2014) Biodegradation of decabromodiphenyl ether (BDE-209) by white-rot fungus *Phlebia lindtneri*. *Chemosphere* 110:70–77
- Ye JS, Yin H, Peng H, Bai JQ, Xie DP, Wang LL (2013a) Biosorption and biodegradation of triphenyltin by *Brevibacillus brevis*. *Bioresour Technol* 129:236–241
- Ye JS, Yin H, Xie DP, Peng H, Huang J, Liang WY (2013b) Copper biosorption and ions release by *Stenotrophomonas maltophilia* in the presence of benzo[a]pyrene. *Chem Eng J* 219:1–9
- Yen JH, Liao WC, Chen WC, Wang YS (2009) Interaction of polybrominated diphenyl ethers (PBDEs) with anaerobic mixed bacterial cultures isolated from river sediment. *J Hazard Mater* 165:518–524
- Yu LH, Luo XJ, Wu JP, Liu LY, Song J, Sun QH, Zhang XL, Chen D, Mai BX (2011) Biomagnification of higher brominated PBDE congeners in an urban terrestrial food web in north China based on field observation of prey deliveries. *Environ Sci Technol* 45:5125–5131
- Zhao Q, Ovchinnikova K, Chai BH, Yoo H, Magula J, Pollack GH (2009) Role of proton gradients in the mechanism of osmosis. *J Phys Chem B* 113:10708–10714
- Zorbas YG, Kakuris KK, Federenko YF, Deogenov VA (2010) Utilization of magnesium during hypokinesia and magnesium supplementation in healthy subjects. *Nutrition* 26:1134–1138